THE ARCHIVE OF MECHANICAL ENGINEERING

Vol. XLVII 2000 Number 4

Key words: *boundary layer flow, rotating sphere, large injection, magnetic field*

MAHESH KUMARI[*)], *GIRISHWAR NATH*[*)]

COMPRESSIBLE BOUNDARY LAYER FLOW IN THE STAGNATION REGION OF A ROTATING SPHERE WITH LARGE INJECTION RATES AND A MAGNETIC FIELD

The effect of large injection rates on the steady laminar compressible boundary layer in the front stagnation-point region of a rotating sphere with a magnetic field has been studied. The effect of variable gas properties, non-unity Prandtl number and viscous dissipation are included in the analysis. The nonlinear coupled ordinary differential equations governing the flow are first linearized using the quasilinearization technique, and the resulting system of linear equations are then solved using an implicit finite-difference scheme with non-uniform step size. For large injection rates, analytical expressions for the surface shear stresses in the longitudinal and rotating directions and the surface heat transfer are also obtained using an approximate method. For large injection rates, the surface heat transfer tends to zero, but the surface shear stresses in the longitudinal and rotating directions remain finite but small. The surface shear stresses and the surface heat transfer decrease with increasing rate of injection, but they increase with the magnetic field and the rotation parameter. The magnetic field or the rotation parameter induces an overshoot in the longitudinal velocity profile and the magnitude of the velocity overshoot increases significantly with the rotation parameters and the injection parameter. The location of the dividing streamline moves away from the boundary with increasing injection rate, but it moves towards the boundary with increasing magnetic and rotation parameters.

Nomenclature

a - velocity gradient at the stagnation point,
B - magnetic field,
$C_f, \overline{C}_f$ - skin friction coefficients in x and y directions,
c_p - specific heat at a constant pressure,

[*)] *Department of Mathematics, Indian Institute of Science, Bangalore, 560 012, India; E-mail: mkumari@math.iisc.ernet.in*

d - step size,
E - electric field,
E_x, E_y, E_z - electric field components along x-, y- and z-directions, respectively,
Ec - viscous dissipation parameter,
$f'(= F)$ - dimensionless velocity component in x-direction,
$f_w (< 0)$ - injection parameter,
F_x, F_y, F_z - magnetic force (Lorentz force) components along x-, y- and z-directions, respectively,
g - dimensionless total enthalpy,
h, H - specific and total enthalpies, respectively,
Ha_x^2 - Hartmann number,
J_x, J_y, J_z - current density components along x-, y- and z-directions, respectively,
L - characteristic length,
M - magnetic parameter which is the ratio of Hartmann number to Reynolds number,
Ma - Mach number,
n - index in the power-law variation of the electrical conductivity,
Pr - Prandtl number,
Pr_m - magnetic Prandtl number,
Re_m - magnetic Reynolds number,
Re_x - Reynolds number,
s - dimensionless velocity along y-direction,
St - Stanton number,
T - temperature,
u, v, w - velocity components along x-, y- and z-directions, respectively,
V - characteristic velocity,
x, y, z - longitudinal, rotational and normal directions, respectively,
γ - ratio of specific heats,
η - transformed independent variable,
λ - rotation parameter,
ρ - fluid density,
μ - coefficient of viscosity,
μ_e^* - magnetic permeability at the edge of the boundary layer,
ν - kinematic viscosity,
σ - electrical conductivity,
Φ - ratio of the density-viscosity product across the boundary layer,
ω - index in the power-law variation of the viscosity,

Ω - angular velocity of the sphere.

Subscripts

e, w - condition at the edge of the boundary layer and on the surface, respectively,

x, z - partial derivative with respect to x and z, respectively.

Superscripts

$'$ (prime) - derivative with respect to η.

1. Introduction

The flow and heat transfer characteristics of spinning bodies of revolution in a forced flow field are important for projectiles or re-entry missiles as well as for certain other engineering problems such as fibre coating, rotating machinery design etc. The increasing use of the blunt bodies in hypersonic flight problems requires accurate prediction of aerodynamic heating at the forward stagnation point, because maximum heat transfer occurs there. When a blunt body moves through the atmosphere at hypersonic speed, the flow field between the body and the detached shock wave is non-viscous in the outer region and viscous in the boundary layer region near the wall. The free stream flow is generally electrically nonconducting, but the flow between the body and the shock wave is conducting due to the ionization of the gas by large temperature rise across the shock wave. It is found that the application of a transverse magnetic field significantly affects the flow field and heat transfer. Also the incorporation of magnetic field coils in space vehicles has got some interesting applications such as opening of communication windows, enhanced flexibility of maneuvers by virtue of flight control, active shielding against radiation etc. [1].

The heat transfer can considerably be reduced by injecting a large amount of fluid from the surface of the body into the boundary layer. The study of boundary layers with large surface injection is required in several applications such as the stagnation region of heat shield protection system for planetary atmospheric probe [2], [3], [4]. When a large amount of fluid is injected into the boundary layer, the injected fluid simply fills the region near the wall and causes significant alteration in the profiles of the flow variables. In such a situation, the boundary layer is characterized by (I) a thick inner layer close to the surface, where viscous forces are negligible compared with the pressure and inertia forces and (II) a relatively thin outer layer in which the transition from the inner to the inviscid external flow takes place. In the inner region, the gradients of the velocity components and enthalpy at the wall are very small, but in the outer region these gradients are large.

In view of the importance of large injection rates on blunt bodies, the steady compressible laminar boundary layer in the front stagnation-point region of a

two-dimensional and axisymmetric bodies with large surface injection rates has been studied by Kubota and Fernandez [5], Kassoy [6], [7], Garett et al. [8], Liu and Nachtsheim [9] and Liu and Chiu [10]. Libby and Cresci [11] have experimentally shown that even for large injection rates the inviscid flow in the stagnation-point region is not affected and therefore the boundary layer concept can be applied to study the effect of large injection rates on the stagnation-point flow without introducing any appreciable error in the analysis. Vigdorovich and Levin [12] have presented an excellent review of literature dealing with large injection rates [12]. The effect of the magnetic field on two-dimensional and axisymmetric stagnation-point flows with or without mass transfer has been investigated by a number of research workers [13], [14], [15], [16], [17], [18], [19], [20], [21], [22], [23], [24]. The flow and heat transfer for the steady boundary layer flow on a rotating sphere have also been considered by several investigators [25], [26], [27], [28], [29], [30], [31]. Also Dorfman [32] and Kreith [33] have presented an excellent review of work done prior to 1958 and 1968, respectively.

For simplicity, the above authors have made some simplifying assumptions such as constant fluid properties ($\rho\mu = \text{constant}$, where ρ and μ are the fluid density and viscosity, respectively), unity Prandtl number ($\text{Pr} = 1$) within the boundary layer, and they have also neglected the viscous dissipation term. The engineering problems mentioned above are characterized by (I) a large temperature difference across the boundary layer, (II) a high free stream Mach number and (III) a large surface injection. These features put constraints on the simplifying assumptions mentioned above for obtaining solutions of the governing equations. A large temperature difference implies that the assumption of a constant density-viscosity product across the boundary layer is not appropriate and more realistic variation of the gas property should be used. For the case of high Mach number, the assumption of unit Prandtl number is not appropriate, because viscous dissipation effects are over simplified. Frictional heating occurs whenever velocity gradients exist in flow of viscous fluids. The effect of viscous dissipation is to augment heat transfer when the surface is cooled and to inhibit heat transfer when the surface is heated. The frictional heating is particularly important in hypersonic and supersonic flows.

It may be remarked that for large injection rates the structure of the boundary layer is quite different from that of moderate or zero injection rates. The structure of the boundary layer for large injection rates is mentioned earlier. For large injection rates, the velocity and temperature gradients are very small and range of integration is large because boundary layer becomes thick. In such a situation, the usual methods for solving the two-point boundary-value problem completely break down due to poor converge and instability of the numerical methods used. Several methods have been used in the past for solving problems involving large injection rates such as the method of matched asymptotic expansion [5], [6], [7], matrix method [8], backward shooting method [9] and an

implicit finite-difference scheme in combination with the quasilinearization technique [10]. For large injection rates, the matrix method becomes unstable. The backward shooting method takes long computing time, which increases as the injection rate increases. The method of matched asymptotic expansion and the implicit finite-difference scheme in combination with the quasilinearization technique are found to very efficient for problems with large injection rates. However, the method of matched asymptotic expansion is an approximate method and to test its accuracy the results have to be compared with the numerical results.

In this investigation, we consider the effect of large injection rates on the steady laminar compressible boundary layer flow of an electrically conducting fluid in the forward stagnation-point region of a rotating sphere with a magnetic field. We have included variable gas properties, non-unity Prandtl number and viscous dissipation terms in our analysis. The coupled nonlinear partial differential equations governing the flow have been reduced to a system of nonlinear coupled ordinary differential equations by similarity transformations. These equations have been solved numerically using an implicit finite-diffrence scheme in combination with the quasilin earization technique. For large injection rates, analytical expressions for surface shear stresses in the longitudinal and rotating directions and the surface heat transfer are found using an approximate method. Particular cases of the present results are compared with those of Sparrow et al. [16], Bush [14], Muthanna and Nath [21], Kubota and Fernandez [5], Liu and Nachtsheim [9], Liu and Chiu [10] and Krishnaswamy and Nath [22].

It may be mentioned that the boundary layer analysis is not strictly applicable to the high energy viscous shock layer type of flow field because there is no asymptotic approach of the velocity profile to some edge value due to the occurrence of strong shock (i.e., $u \to u_s$ instead of $u \to u_e$). However, there is a shear layer edge within the shock layer where the specific enthalpy $h \to h_e$ [14], [19]. In spite of this short coming, the present study will exhibit most of the characteristics of flow and enthalpy fields and can form the basis for further analysis with more realistic models.

2. Problem formulation

To fix the problem mathematically, an orthogonal curvilinear coordinate system is considered in which x measures the distance along the meridian from the forward stagnation point, y represents the distance in the direction of rotation, z is the distance normal to the body, and $r(x)$ is the normal distance of a point on the body from the axis of rotation and it is nearly equal to x in the vicinity of the stagnation point (Fig. 1). We consider the steady laminar compressible boundary layer flow of an electrically conducting fluid in the forward stagnation point region of a rotating sphere with a magnetic field B

applied in z-direction and fixed relative to the fluid. We take the gas with variable properties ($\rho\alpha T^{-1}$, $\mu\alpha T^{\omega}$, $\sigma\alpha T^{n}$). It is assumed that the magnetic Reynolds number $\mathrm{Re}_m = \mu_e^* \sigma_e VL << 1$. Under this condition it is possible to neglect the effect of the induced magnetic field. It is also assumed that there is no applied or polarization voltage which implies that the electric field $\vec{E} = 0$ [34]. Rathbun [35] has also discussed this aspect in detail and has shown that the assumption $\vec{E} = 0$ is valid provided the magnetic Prandtl number $\mathrm{Pr}_m = \mu_e^* \sigma_e \nu_e \leq 10^{-5}$. This condition is met in most applications. Hence the electric field $\vec{E}$ is not included in the relevant equations. This corresponds to the case where no energy is added to or extracted from the fluid by electrical means.

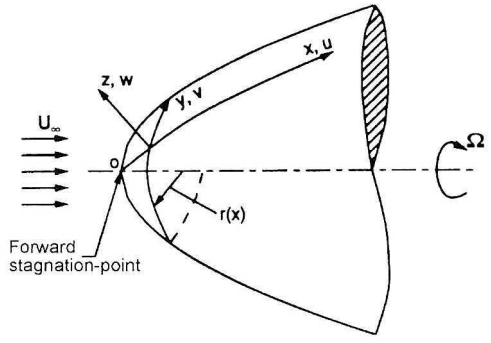

Fig. 1. Physical model and co-ordinate system

The electrical current flowing in the fluid will give rise to induced magnetic field which would exist if the fluid were an electrical insulator. Here we have taken the fluid to be electrically conducting. Since $\mathrm{Pr}_m << 1$, the magnetic boundary layer is much thicker than the viscous boundary layer. This provides further justification for ignoring the induced electric and magnetic fields within the viscous boundary layer [16]. Under these assumptions it is possible to show that only the applied magnetic field contributes to the magnetic force (Lorentz force). The magnetic force components in x-, y- and z-directions are given by $F_x = J_y B = \sigma(E_y - B^2 u)$, $F_y = -J_x B = -\sigma(E_x + B^2 v)$, $F_z = 0$, where $J_x = \sigma(E_x + Bv)$, $J_y = \sigma(E_y - Bu)$, $J_z = \sigma E_z$. As mentioned earlier, the electric field can be neglected. Hence $E_x = E_y = E_z = 0$. Consequently $F_x = -\sigma B^2 u$, $F_y = -\sigma B^2 v$, $F_z = 0$. The Hall effect is neglected. The wall and free stream total enthalpies are taken as constants. Under the above mentioned assumptions, the boundary layer equations governing the steady compressible flow in the vicinity of a forward stagnation point of a rotating sphere with an applied magnetic field are given by [14], [16], [21], [26], [36]

$$(\rho x u)_x + (\rho x w)_z = 0\,, \tag{1}$$

$$\rho(uu_x + wu_z - v^2/x) = \rho_e u_e (u_e)_x + (\mu u_z)_z - B^2(\sigma u - \sigma_e u_e)\,, \tag{2}$$

$$\rho(uv_x + wv_z + uv/x) = (\mu v_z)_z - \sigma B^2 v, \tag{3}$$

$$\rho(uH_x + wH_z) = [\mathrm{Pr}^{-1}\,\mu H_z]_z - [\mu(\mathrm{Pr}^{-1} - 1)(uu_z + vv_z)]_z\,. \tag{4}$$

The boundary conditions are

$$z = 0,\ x \geq 0 \ :\ u = 0,\ v = \Omega x,\ w = w_w,\ H = H_w\,,$$

$$z \to \infty,\ x \geq 0 \ :\ u = u_e(x),\ v = 0,\ H = H_e\,,$$

$$x = 0,\ z > 0 \ :\ u = u_e(x),\ v = 0,\ H = H_e\,. \tag{5}$$

In order to reduce the partial differential equations (1)-(4) to ordinary differential equations in dimensionless form, we apply the following transformations

$$\eta = (2a/\nu_e)^{1/2}\int_0^z (\rho/\rho_e)dz,\ u = u_e f'(\eta),\ v = \Omega x s(\eta)\,,$$

$$H = H_e g(\eta),\ H = h + 2^{-1}(u^2 + v^2), h/h_e = (1 - Ec)^{-1}[g - Ec(f'^2 + \lambda s^2)],\ Ec < 1,$$

$$\lambda = (\Omega/a)^2,\ \rho_e/\rho = T/T_e = h/h_e,\ \mu/\mu_e = (T/T_e)^{\omega} = (h/h_e)^{\omega}\,,$$

$$\Phi = (\rho\mu)/(\rho\mu)_e = (h/h_e)^{\omega - 1},\ \sigma/\sigma_e = (T/T_e)^n = (h/h_e)^n\,,$$

$$M = \sigma_e B^2 x/\rho_e u_e = Ha_x^2/\mathrm{Re}_x,\ u_e = ax, \tag{6}$$

$$Ha_x^2 = \sigma_e B^2 x^2/\mu_e,\ \mathrm{Re}_x = ax^2/\nu_e\,,$$
$$Ec = u_e^2/(2H_e) = [(\gamma - 1)Ma_e^2/2]/[1 + (\gamma - 1)Ma_e^2/2],$$
$$w = -(2a\nu_e)^{1/2}(\rho_e/\rho)f(\eta)\,,$$

$$\mathrm{Pr} = \mu c_p/k,\ g > Ec(f'^2 + \lambda s^2) \quad \text{for non-integral } \omega \text{ and } n\,,$$

to these equations and we find that Eq. (1) is identically satisfied and Eqs. (2)-(4) reduce to

$$(\Phi f'')' + ff'' + 2^{-1}[(\rho_e/\rho) - f'^2 + \lambda s^2] + 2^{-1}M(\rho_e/\rho)[1 - (\sigma/\sigma_e)f'] = 0\,, \tag{7}$$

$$(\Phi s')' + fs' - f's - 2^{-1}M(\sigma/\sigma_e)(\rho_e/\rho)s = 0\,, \tag{8}$$

$$(\mathrm{Pr}^{-1}\Phi g')' + fg' - 2Ec[\Phi(\mathrm{Pr}^{-1} - 1)(ff'' + \lambda ss')]' = 0\,, \tag{9}$$

where Φ, ρ_e/ρ, and σ/σ_e are given by (6) and are functions of g, f' and s. The boundary conditions are given by

$$f(0)=f_w,\ f'(0)=0,\ s(0)=1,\ g(0)=g_w,\\ f'(\infty)=1,\ s(\infty)=0,\ g(\infty)=1, \tag{10}$$

where

$$f_w=-2^{-1/2}(\mathrm{Re}_x)^{1/2}(\rho w)_w/(\rho u)_e,\quad \mathrm{Re}_x=u_e x/\nu_e. \tag{11}$$

If the normal velocity at the surface $(w)_w$ is selected in such a manner that $(\rho w)_w/(\rho u)_e$ is a constant, then f_w will be a constant provided Re_x, is fixed. For injection $f_w<0$, it is assumed that the injected gas possesses the same physical properties as the boundary layer gas and has a temperature equal to the wall temperature. Both gases are assumed to have same physical properties.

It may be noted that the parameter $\omega=0.7$ corresponds closely to low temperature flows and $\omega=0.5$ represents conditions encountered in hypersonic flight. The value $\omega=1(\Phi=1)$ represents the simplification of constant density-viscosity product across the boundary layer [37]. The variation of the Prandtl number Pr in the boundary layer for most atmospheric flight is less than 5 per cent [38]. Hence as a first approximation Pr is taken as a constant across the boundary layer. This assumption is not expected to introduce appreciable error in the solution and at the same time the governing equations are simpler to handle. In the vicinity of the stagnation point Ec can be taken as locally constant for a prescribed Mach number Ma_e.

It may be remarked that Eqs. (7) and (9) for $\lambda=f_w=Ec=0$, $\omega=\Phi=\mathrm{Pr}=1$ reduce to those of Bush [14], for $\lambda=Ec=0$, to those of Muthanna and Nath [21] and Krishnaswamy and Nath [22], for $\lambda=Ec=M=0$, $\omega=\Phi=\mathrm{Pr}=1$ to those of Kubota and Fernandez [5], Liu and Nachtsheim [9] and Liu and Chiu [10], and for $\lambda=Ec=0$, $\omega=\Phi=\sigma/\sigma_e=\rho_e/\rho=1$ to those of Sparrow et al. [16].

The skin friction coefficients in the longitudinal direction (x-direction) and rotating direction (y-direction) and the heat transfer coefficient in terms of Stanton number are given by

$$C_f=2(\mu\ \partial u/\partial z)_w/\rho_e u_e^2=2^{3/2}(\mathrm{Re}_x)^{-1/2}\Phi_w f_w'',$$

$$\overline{C}_f=2(\mu\,\partial v/\partial z)_w/\rho_e u_e^2=2^{3/2}(\mathrm{Re}_x)^{-1/2}\lambda^{1/2}\Phi_w s_w', \tag{12}$$

$$St=(\mu\,\partial H/\partial z)_w/[\rho_e u_e(H_e-H_w)]=(\mathrm{Re}_x/2)^{-1/2}\Phi_w(1-g_w)^{-1}g_w'.$$

3. Numerical method

Eqs. (7)-(9) under boundary conditions (10) are first linearized using the quasilinearization technique [37], [38] and the resulting system of linear ordinary differential equations is solved numerically using an implicit

finite-difference scheme with variable grid size. The method is essentially similar to that of Liu and Chiu [10]. Hence the method is not described here.

4. Approximate solution

It is possible to obtain analytical expressions for surface shear stresses and surface heat transfer when the injection rate is large ($f_w \to \infty$). It is convenient to change both the independent and dependent variables in Eqs. (7)-(9) and they are given by

$$\xi = \eta/(-f_w), \quad f(\eta) = (-f_w) f_1(\xi), \quad s(\eta) = s_1(\xi), \quad g(\eta) = g_1(\xi), \quad \varepsilon = 1/(-f_w)^2, \quad f_w < 0. \tag{13}$$

Using (13), Eqs. (7)-(9) are transformed to

$$\varepsilon \frac{d}{d\xi}\left(\Phi \frac{d^2 f_1}{d\xi^2}\right) + f_1 \frac{d^2 f_1}{d\xi^2} + 2^{-1}\left[\frac{\rho_e}{\rho} - \left(\frac{df_1}{d\xi}\right)^2 + \lambda s_1^2\right] + 2^{-1} M \left(\frac{\rho_e}{\rho}\right)\left[1 - \left(\frac{\sigma}{\sigma_e}\right)\frac{df_1}{d\xi}\right] = 0 \tag{14}$$

$$\varepsilon \frac{d}{d\xi}\left(\Phi \frac{ds_1}{d\xi}\right) + f_1 \frac{ds_1}{d\xi} - \frac{df_1}{d\xi} s_1 - 2^{-1} M \left(\frac{\sigma}{\sigma_e}\right)\left(\frac{\rho_e}{\rho}\right) s_1 = 0, \tag{15}$$

$$\varepsilon \frac{d}{d\xi}\left(\Phi \frac{dg_1}{d\xi}\right) + \Pr f_1 \frac{dg_1}{d\xi} - \varepsilon Ec \frac{d}{d\xi}\left[2\Phi(1-\Pr)\left(\frac{df_1}{d\xi}\frac{d^2 f_1}{d\xi^2} + \lambda s_1 \frac{ds_1}{d\xi}\right)\right] = 0, \tag{16}$$

where

$$\Phi = (1 - Ec)^{1-\omega}\left[g_1 - Ec\left\{(df_1/d\xi)^2 + \lambda s_1^2\right\}\right]^{\omega - 1},$$

$$\rho_e/\rho = (1 - Ec)^{-1}\left[g_1 - Ec\left\{(df_1/d\xi)^2 + \lambda s_1^2\right\}\right], \tag{17}$$

$$\sigma/\sigma_e = (1 - Ec)^{-n}\left[g_1 - Ec\left\{(df_1/d\xi)^2 + \lambda s_1^2\right\}\right]^n.$$

The boundary conditions (10) can be written as

$$f_1 = -1, \quad df_1/d\xi = 0, \quad s_1 = 1, \quad g_1 = g_w \quad \text{at} \quad \xi = 0, \tag{18a}$$

$$df_1/d\xi \to 1, \quad s_1 \to 0, \quad g_1 \to 1 \quad \text{as} \quad \xi \to \infty. \tag{18b}$$

It may be remarked that the highest derivative in Eqs. (14)-(16) is multiplied by a small parameter ε. Hence the order of these equations are reduced as $\varepsilon \to 0$ ($f_w \to \infty$). Such a problem is obviously a singular perturbation problem. As $\varepsilon \to 0$, Eqs. (14)-(16) reduce to

$$f_1 \frac{d^2 f_1}{d\xi^2} + 2^{-1}\left[\frac{\rho_e}{\rho} - \left(\frac{df_1}{d\xi}\right)^2 + \lambda s_1^2\right] + 2^{-1} M \left(\frac{\rho_e}{\rho}\right)\left[1 - \left(\frac{\sigma}{\sigma_e}\right)\frac{df_1}{d\xi}\right] = 0, \tag{19}$$

$$f_1 \frac{ds_1}{d\xi} - \frac{df_1}{d\xi} s_1 - 2^{-1} M \left(\frac{\sigma}{\sigma_e} \right) \left(\frac{\rho_e}{\rho} \right) s_1 = 0 , \tag{20}$$

$$f_1 \frac{dg_1}{d\xi} = 0 . \tag{21}$$

The boundary conditions for Eqs. (19)-(21) are given by (18a). As Eqs. (19)-(21) are valid only near the wall, the conditions at infinity given by (18b) are discarded. It may be noted that Eqs. (19)-(21) are independent of the parameter ω characterising the variation of the density-viscosity product across the boundary layer and the Prandtl number Pr. This is expected as these parameters are associated with the viscosity of the fluid. For large injection rates normal to the surface, the fluid near the wall, as a first approximation, may be regarded as inviscid and rotational [5], [7]. In Eqs. (19)-(21) $f_1 = -1$ on the surface (i.e., at $\xi = 0$) and it increases monotonically with ξ and becomes zero at $\xi = \xi_0$ (i.e., $f_1(\xi_0) = 0$). It may be noted that $\xi = \xi_0$ represents the location of the dividing streamline separating the inviscid flow from the oncoming flow [9]. Hence Eqs. (19)-(21) become singular at $\xi = \xi_0$. Since Eqs. (19)-(21) are valid near the wall (i.e., near $\xi = 0$), they could be solved numerically. However, we are interested in surface shear stresses in x and y directions and surface heat transfer and they can be obtained from Eqs. (19)-(21). From Eq. (21),

$$dg_1 / d\xi = 0 \qquad \text{for all } \xi , \tag{22a}$$

and using the condition on g_1 in (18a), we get

$$g_1 = g_w \quad \text{for all. } \xi . \tag{22b}$$

Using (22b), and the conditions on f_1 and s_1 in Eq. (18a), we get the velocity gradients in the x and y directions on the surface

$$\frac{d^2 f_1}{d\xi^2}(0) = 2^{-1}(1+M)(1-Ec)^{-1}(g_w - \lambda Ec) + 2^{-1}\lambda , \tag{23a}$$

$$\frac{ds_1}{d\xi}(0) = -2^{-1} M (1-Ec)^{-(1+n)} (g_w - \lambda Ec)^{1+n} . \tag{23b}$$

The surface shear stresses in the x and y directions and the surface heat transfer are expressed as

$$f''(0) = \left(\frac{d^2 f_1}{d\xi^2}(0) \right) \Big/ (-f_w) = 2^{-1}\left[(1+M)(1-Ec)^{-1}(g_w - \lambda Ec) + \lambda\right]/(-f_w),$$

$$s'(0)=\left(\frac{ds_1}{d\xi}(0)\right)\Big/(-f_w)=-2^{-1}\,M(1-Ec)^{-(1+n)}(g_w-\lambda Ec)^{1+n}/(-f_w), \quad (24)$$

$$g'(0)=\left(\frac{dg_1}{d\xi}(0)\right)\Big/(-f_w), \quad g_w > Ec \text{ where n is non-integral.}$$

It is evident from the above equations that for large injection rates, the surface heat transfer $g'(0)$ vanishes, but the surface shear stresses in the longitudinal and rotational directions $(f''(0),-s'(0))$ remain finite. The surface shear stresses $(f''(0),-s'(0))$ vary inversely as $(-f_w)$ and directly as M and g_w. They also depend on λ, Ec and n.

5.Results and discussion

Eqs. (7)-(9) under boundary conditions (10) were solved numerically using an implicit finite-difference with variable step size in combination with the quasilinearization technique [10], [39], [40]. The computations were carried out for various values of the parameters $M\ (0\le M\le 20)$, $-f_w\ (0\le -f_w\le 30)$, $\lambda\ (0\le\lambda\le 10)$, $\omega\ (0.5\le\omega\le 1)$, $g_w\ (0.2\le g_w\le 0.6)$, $Ec\ (0\le Ec\le 0.8)$, $n\ (0.5\le n\le 1.5)$ and $\Pr=0.72$. However, for the sake of brevity, only some representative results are presented.

In order to validate our results we have compared our surface shear stress in x-direction $(f''(0))$ and the surface heat transfer $(g'(0))$ for $f_w=Ec=\lambda=0$, $\omega=\Pr=1$, $g_w=0.05$ with those of Bush [14], for $f_w=Ec=\lambda=0$, $\omega=0.5$, $\Pr=0.72$, $g_w=0.2,0.6$ with those of Muthanna and Nath [21], for $Ec=\lambda=0$, $\omega=0.5$, $\Pr=0.72$, $g_w=0.6$ with those of Krishnaswamy and Nath [22] and for $Ec=\lambda=0$, $\rho_e/\rho=\omega=1$, $\Pr=0.7$ with those of Sparrow et al. [16] and found them in excellent agreement. The maximum difference is found to be less than 0.2 per cent. Since the results are tabulated in [14], [16], [21], [22], for the sake of brevity, the comparison is not presented here. Also for moderate injection rate, we have compared the velocity profile in x-direction (f') and the total enthalpy profile (g) for $\lambda=Ec=M=0$, $f_w=-2$, $g_w=0.5$, $\omega=\Pr=1$ with those of Kubota and Fernandez [5]. For large injection rate, we have compared the velocity profile in x-direction (f') and the total enthalpy profile $(1-g)$ for $M=\lambda=Ec=0$, $f_w=-10$, $g_w=0.5$, $\omega=\Pr=1$ with those of Liu and Nachtsheim [9] and for $M=\lambda=Ec=0$, $f_w=-30$, $g_w=0.25$, $\omega=\Pr=1$ with those of Liu and Chiu [10]. In all the cases the results were found to be in very good agreement. The comparison is shown in Figs. 2-4.

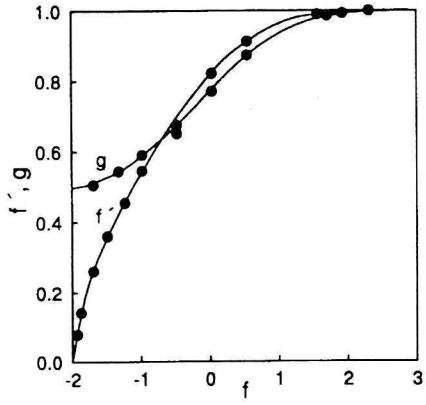

Fig. 2. Comparison of the velocity profile (f') and the total enthalpy profile (g) for $\lambda = M = Ec = 0$, $f_w = -2$, $g_w = 0.5$, $\omega = \Pr = 1$, _____, Present results; • Kubota and Fernandez

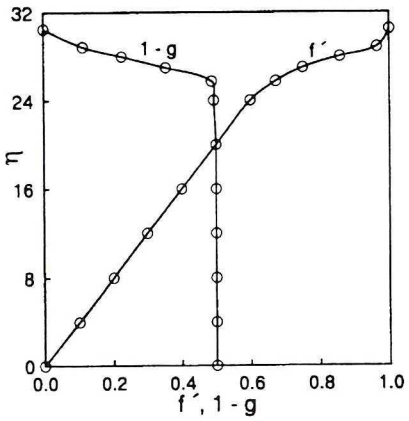

Fig. 3. Comparison of the velocity profile (f') and the total enthalpy profile ($1-g$) for $\lambda = M = Ec = 0$, $f_w = -10$, $\omega = \Pr = 1$, $g_w = 0.5$, _____, Present results; o, Liu and Nachtsheim

We have compared the surface shear stresses in the longitudinal and rotating directions $(f''(0), -10s'(0))$ for $M = 5,\ 10$, $\lambda = \omega = n = 1$, $g_w = 0.6$, $Ec = 0.5$, $\Pr = 0.72$, $3 \le -f_w \le 60$ obtained by the asymptotic and numerical methods and we find that they agree very well for $-f_w \ge 5$. The comparison is shown in Fig. 5.

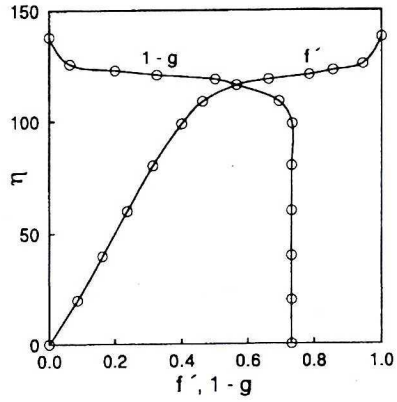

Fig. 4. Comparison of the velocity profile (f') and the total enthalpy profile ($1-g$) for $\lambda = M = Ec = 0$, $f_w = -30$, $\omega = \Pr = 1$, $g_w = 0.5$, _____, Present results; o, Liu and Chiu

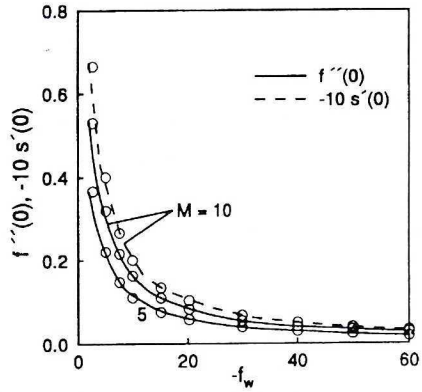

Fig. 5. Comparison of the surface shear stress in the longitudinal and rotating directions ($f''(0), -s'(0)$) for $M = 5,10$, $\lambda = n = \omega = 1$, $g_w = 0.6$, $\Pr = 0.72$, $Ec = 0.5$, $3 \le -f_w \le 60$, _____, Numerical; o, Asymptotic

The effect of the magnetic parameter (M) on the velocity profiles in x- and y-directions (f', s) and the total enthalpy profiles (g) with variable electrical conductivity ($\sigma/\sigma_e = (T/T_e)^n$) for $f_w = -10$, $\lambda = 5$, $Ec = 0$, $g_w = 0.6$, $\omega = 0.5$, $\Pr = 0.72$, $n = 1$ is presented in Fig. 6. It can be seen from the figure that for variable electrical conductivity the magnetic parameter (M) induces an overshoot in the velocity profile in x-direction (f') near the wall and the magnitude of the overshoot increases with M. The physical explanation for the velocity overshoot is as follows. For cool walls ($g_w < 1$), the enthalpy profile (g) corresponding to the case of variable electrical conductivity will lie above that calculated for a constant value. In this case the mass density is lowered.

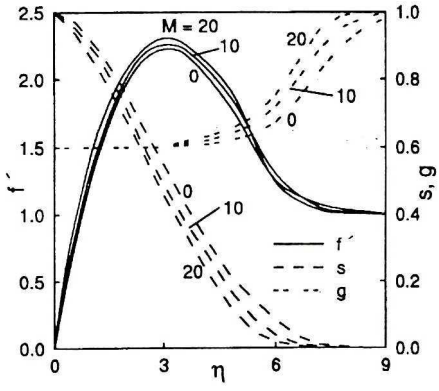

Fig. 6. Effect of the magnetic parameter M on the velocity profiles in x and y directions (f', s) and the total enthalpy profile (g) for $f_w = -10$, $\lambda = 5$, $Ec = 0$, $g_w = 0.6$, $\omega = 0.5$, $\Pr = 0.72$, $n = 1$, _____, f'; — — —, s; – – – – – –, g

Hence the flow accelerates resulting in velocity above that prevailing at the edge of the boundary layer [15]. Also there is velocity overshoot in the velocity f' even when $M = 0$ .This is due to the rotation parameter λ as will be explained later. There is no velocity overshoot for $\lambda = M = 0$. Thus the velocity overshoot in f' is due to either magnetic field with variable electrical conductivity or due to the rotation parameter. The magnetic field gives rise to a magnetic force in the rotating direction (y-direction) which tends to oppose the fluid motion. This causes reduction in the velocity in y-direction (s). The velocity profile in z-direction (f) increases with increasing magnetic field. Hence the total enthalpy profile (g) is increased.

The effect of the rotation parameter (λ) on the velocity profiles in the longitudinal and rotating directions (f', s) and the total enthalpy profile (g) for $f_w = -10$, $g_w = 0.2$, $\omega = 0.5$, $M = 10$, $Ec = 0$, $\Pr = 0.72$, $n = 1$ is displayed in Fig. 7. There is a velocity overshoot in the longitudinal velocity profile (f') caused by the rotation parameter (λ) and the velocity overshoot increases with λ. Similar trend has been observed by Back [41] while considering the rotating flow over a stationary surface. The reason for the velocity overshoot in f' is that the flow within and outside the boundary layer is acted upon the same pressure gradient $-dp/dx = \rho_e u_e du_e/dx + \sigma_e B^2 u_e$. However, in the boundary layer, viscous effects reduce the tangential velocity (v) and thus the acceleration term $(\rho v^2/x)$. Consequently, the longitudinal pressure gradient $(-dp/dx)$ induces larger longitudinal flow acceleration to occur in the boundary layer than that present without the tangential velocity (v) even though the shear stress tends to balance the longitudinal pressure gradient near the wall [39]. Hence the velocity overshoot occurs in f' when $\lambda > 0$ and it increases with λ. Also, the velocity profile in y-direction (s) decreases everywhere as the rotation parameter λ increases. The increase in λ enhances the relative velocity between the wall and the fluid which in turn reduces the boundary layer

thickness. Consequently, the velocity s is lowered with the increase in the rotation parameter λ. Since the velocity in the normal direction (f) is increased with the rotation parameter which causes reduction in the thermal boundary layer thickness, the total enthalpy profile (g) is increased.

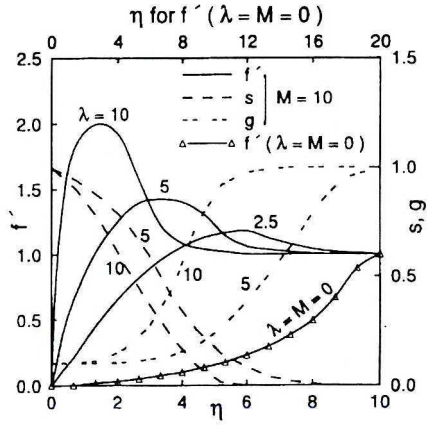

Fig. 7. Effect of the rotation parameter λ on the velocity profiles in x and y directions (f', s) and the total enthalpy profile (g) for $f_w = -10$, $g_w = 0.2$, $\omega = 0.5$, $M = 10$, $\mathrm{Pr} = 0.72$, $n = 1$, $Ec = 0$, _____, f'; — — —, s; – – – – – –, g

The effect of large injection rate $(-f_w > 3)$ on the velocity profiles in the longitudinal and rotating directions (f', s) and the enthalpy profile (g) is presented in Figs. 8 and 9. It is evident from these figures that for large injection rates, there is essentially no heat transfer, but there is still a certain amount of frictional drag on the body. The velocity and thermal boundary layer thicknesses increase significantly with the injection rate.

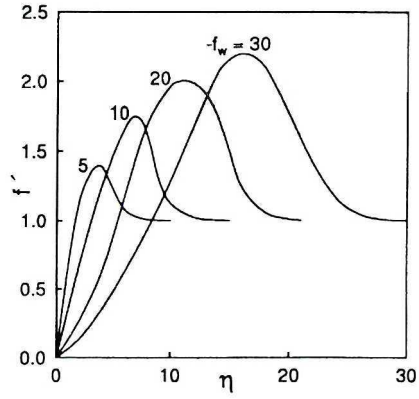

Fig. 8. Effect of the injection parameter (f_w) on the velocity profile in x direction (f') for $M = 10$, $\lambda = 1$, $g_w = 0.6$, $\omega = Ec = 0.5$, $n = 1$, $\mathrm{Pr} = 0.72$

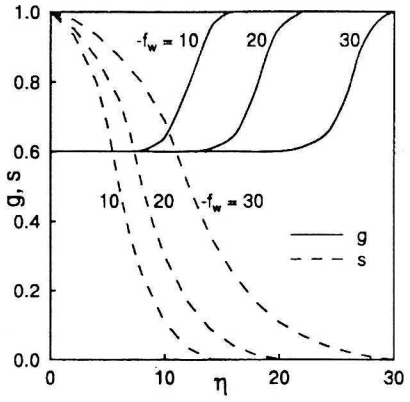

Fig. 9. Effect of the injection parameter (f_w) on the velocity profile in y-direction (s) and the total enthalpy profile (g) for $M = 10$, $\lambda = 1$, $g_w = 0.6$, $\omega = Ec = 0.5$, $n = 1$, Pr = 0.72. _____, g; — — —, s

These figures suggest division of boundary layer into two regions, a practically insulated region near the surface where $g \approx g_w$ and a region in which the variation of g is large. Similar phenomenon has been observed by other investigators [5], [6], [7], [8], [9], [10].

The effect of wall total enthalpy (g_w) on the velocity components (f', s) and the total enthalpy profile (g) is displayed in Fig. 10. The increase in g_w reduces the overshoot in the velocity profile f' as well as the value of the velocity profile s, because the velocity boundary layers increase due to wall heating. The thermal boundary layer also increases with g_w. The physical reason is that for gases the viscosity of the fluid μ increases with temperature which results in thicker velocity and thermal boundary layers.

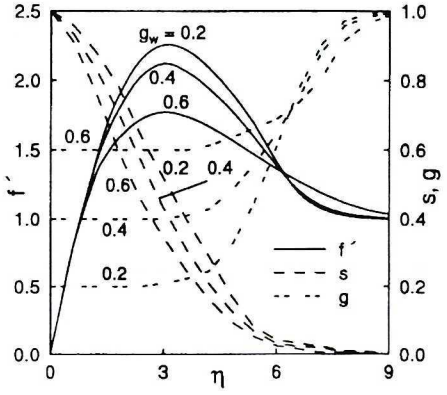

Fig. 10. Effect of the total enthalpy on the wall (g_w) on the velocity profiles in x- and y-directions (f', s) and the total enthalpy profile (g) for $M = 10$, $\lambda = 5$, $f_w = -10$, $\omega = 0.5$, $Ec = 0$, Pr = 0.72, $n = 1$, _____, f'; — — —, s; – – – – – –, g

The effect of the parameter n, which is the index in the power-law variation of the electrical conductivity in the boundary layer, on the velocity and total enthalpy profiles (f', g) is shown in Fig. 11. It can be seen that both velocity and thermal boundary layers reduce as n increases. Hence, the velocity and total enthalpy profiles (f', g) increase with n. However its effect on the velocity s is rather small. Hence it is not shown here.

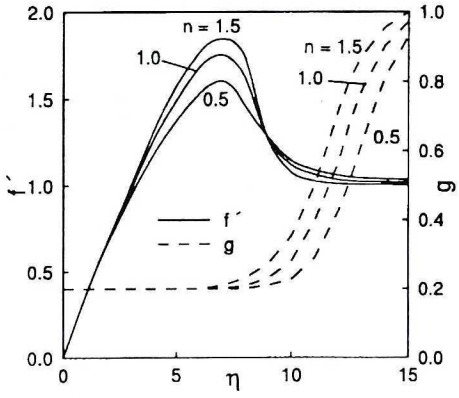

Fig. 11. Effect of the parameter n on the velocity profiles in x-directions (f') and the total enthalpy profile (g) for $M = 10$, $\lambda = 1$, $f_w = -10$, $g_w = 0.6$, $Ec = \omega = 0.5$, $\Pr = 0.72$, ———, f'; — — —, g

The effect of the parameter ω, which characterises the variation of the density-viscosity product across the boundary layer, on the velocity and total enthalpy profiles (f', g) is presented in Fig. 12. The effect of ω on s is rather small and hence it is not shown here.

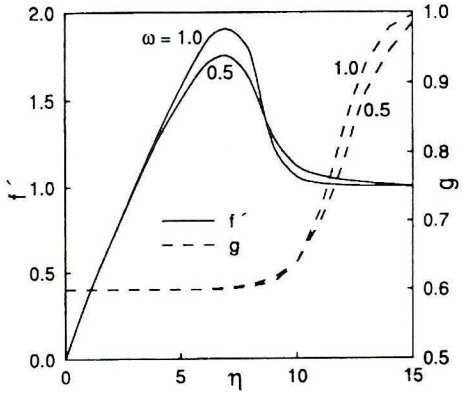

Fig. 12. Effect of the parameter ω on the velocity profiles in x-directions (f') and the total enthalpy profile (g) for $M = 10$, $\lambda = n = 1$, $f_w = -10$, $g_w = 0.6$, $Ec = 0.5$, $\Pr = 0.72$, ———, f'; — — —, g

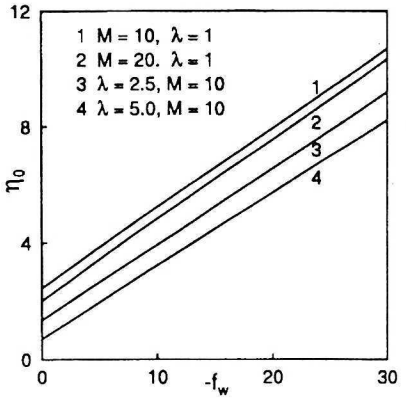

Fig. 13. Effect of the injection parameter $(-f_w)$, the magnetic parameter (M) and the rotation parameter (λ) on the location of the dividing streamline (η_0) for $\omega = 0.5$, $g_w = 0.2$, $Ec = 0$, $\Pr = 0.72$, $n = 1$

Fig. 13 shows the effect of the injection parameter $(-f_w)$, the magnetic parameter (M) and the rotation parameter (λ) on the location of the dividing streamline $(\eta_0$ where $f(\eta = \eta_0) = 0)$ for $\omega = 0.5$, $g_w = 0.2$, $Ec = 0$, $n = 1$, $\Pr = 0.72$. It can be seen from the figure that the injection $(-f_w)$ causes the location of the dividing streamline (η_0) to move away from the boundary, but η_0 moves towards the boundary due to increase in the magnetic and rotation parameters (M, λ). The dividing streamline (η_0) increases almost linearly with the injection parameter $(-f_w)$.

6. Conclusions

For large injection rates, the heat transfer is nearly zero, but there is a certain amount of frictional drag on the body. The velocity and thermal boundary layers increase significantly with the injection rate. Also, for large injection rates the effect of the density-viscosity product across the boundary layer is rather small. The magnetic field in the presence of variable electrical conductivity and the rotation parameter induce overshoot in the velocity profiles in the longitudinal direction and the magnitude of the velocity overshoot increases with injection, rotation and magnetic parameters. The magnetic field and the rotation parameter increase the surface shear stress and heat transfer. For large injection rates, the surface shear stresses and the surface heat transfer obtained by the approximate method are found to be in very good agreement with those of the numerical results. The location of the dividing streamline moves away from the boundary with increasing injection parameter, but it moves towards the boundary due to increasing magnetic and rotation parameters.

* * *

Acknowledgement: One of the authors (MK) is thankful to the University Grants Commission, India, for the financial support under the Research Scientist Scheme.

Manuscript received by Editorial Board, December 28, 1999;
final version, September 29, 2000.

REFERENCES

[1] Nowak R., Kranc S., Porter R.W., Yuen M.C., Cambel A.B.: Magnetogasdynamic re-entry phenomena. J. Spacecraft and Rockets, 4, pp. 1538÷1542, 1967.

[2] Tauber M.E.: Atmospheric entry into Jupiter. J. Spacecraft and Rockets, 6, pp. 1103÷1109, 1969.

[3] Page W.A.: Aerodynamic heating for probe vehicles entering the outer planets. Adv. Astron. Sci., 29, pp. 191÷214, 1971.

[4] Tauber M.E.: Heat protection for atmospheric entry into Saturn, Uranus and Neptune. Adv. Astron. Sci., 29, pp. 215÷228, 1971.

[5] Kubota T., Fernandez F.L.: Boundary-layer flows with large injection and heat transfer. AIAA J., 6, pp. 22÷28, 1968.

[6] Kassoy D.R.: On laminar boundary-layer blow-off. SIAM J.Appl. Math., 18, pp. 29÷40, 1970.

[7] Kassoy D.R.: On laminar boundary-layer blow-off. Part 2. J. Fluid Mech., 48, pp. 209÷228, 1971.

[8] Garett L.B., Smith G.L., Perkins J.N.: An implicit finite-difference solution to the viscous shock layer including the effect of radiation and strong blowing. NASA TR-R, 388, 1972.

[9] Liu T.M., Nachtsheim P.R.: Shooting method for solution of boundary-layer flows with massive blowing. AIAA J., 11, pp. 1584÷1586, 1973.

[10] Liu T.M., Chiu H.H.: Fast and stable numerical method for boundary-layer flow with massive blowing. AIAA J., 14, pp. 114÷116, 1976.

[11] Libby P.A., Cresci R.J.: Experimental investigation of the downstream influence of stagnation-point mass transfer. J. Aerospace Sci., 28, pp. 51÷64, 1961.

[12] Vigdorovich I.I., Levin V.A.: Supersonic flow over bodies in the case of massive blowing. Fluid Mech.-Sov. Res., 13, pp. 31÷68, 1984.

[13] Wu C.S.: Hypersonic viscous flow near the stagnation point in the presence of a magnetic field. J. Aerospace Sci., 27, pp. 892÷893, 1960.

[14] Bush W.B.: The stagnation-point boundary layer in the presence of an applied magnetic field. J. Aerospace Sci., 28, pp. 610÷611, 1961.

[15] Lykoudis P.S.: Velocity overshoots in magnetic boundary layers. J. Aerospace Sci., 28, pp. 896÷897, 1961.

[16] Sparrow E.M., Eckert E.R.G., Minkowycz W.J.: Transpiration cooling in a magnetohydrodynamic stagnation–point flow. Appl. Sci. Res., 11A, pp. 125÷147, 1962.

[17] Smith M.C., Wu C.S.: Magnetohydrodynamic hypersonic viscous flow past a blunt body. AIAA J., 2, pp. 963÷965, 1964.

[18] Smith M.C., Schwimmer H.S., Wu C.S.: Magnetohydrodynamic -hypersonic viscous and inviscid flow near the stagnation point of a blunt body, AIAA J., 3, pp. 1365÷1367, 1965.

[19] Chen S.Y.: Magneto hypersonic flow near the stagnation point at low Reynolds number, J. Spacecraft and Rockets, 6, pp. 872÷877, 1969.

[20] Yoo C.Y., Porter R.W.: Numerical analysis of the viscous, hypersonic MHD blunt-body problem. AIAA J., 11, pp. 383÷384, 1973.

[21] Muthanna M., Nath G.: Magnetic hypersonic rarefied flow at the stagnation point of a blunt body with slip and mass transfer. Int. J. Heat Mass Transfer, 19, pp. 603÷612, 1976.

[22] Krishnaswamy R., Nath G.: Hypersonic stagnation-point boundary layers with massive blowing in the presence of a magnetic field. Phys. Fluids, 22, pp. 1631÷1638, 1979.

[23] Nataraja H.R., Mittal M.L., Rao B.N.: Laminar MHD compressible boundary layer at a wedge. Int. J. Engng. Sci., 24, pp. 1303÷1310, 1986.

[24] Kumari M., Takhar H.S., Nath G.: Compressible MHD boundary layer in the stagnation region of a sphere. Int. J. Engng. Sci., 28, pp. 357÷366, 1990.

[25] Illingworth C.R.: The laminar boundary layer of a rotating body of revoulution. Phil. Mag., 44, pp. 389÷403, 1953.

[26] Scala S.M., Workman J.B.: The stagnation-point boundary layer on a rotating hypersonic body. J. Aerospace Sci., 26, 183, 1959.

[27] Hussaini M.Y., Sastry M.S.: The laminar compressible boundary layer on a rotating sphere with heat transfer. J. Heat Transfer, 98, pp. 533÷535, 1976.

[28] Lee M.H., Jeng D.R., DeWitt K.J.: Laminar boundary layer transfer over rotating bodies in forced flow. J. Heat Transfer, 100, pp. 496÷502, 1978.

[29] Shaarawi M.A.I.Ei., Refaic M.F.Ei., Bedeawi S.A.Ei.: Numerical solution of laminar boundary layer flow about a rotating sphere in an axial stream. J. Fluids Engng., 107, pp. 97÷104, 1985.

[30] Chandran P., Kumar P.: Flow and heat transfer in the boundary layer due to rotating spheres, spheroids and paraboloids. Int. J. Engng. Sci., 24, pp. 685÷701, 1986.

[31] Wang C.Y.: Boundary layers on rotating cones, discs and axisymmetric surface with a concentrated source. Acta Mechanica, 81, pp. 245÷251, 1990.

[32] Dorfman L.A.: Hydromagnetic Resistance and Heat Loss of Rotating Bodies, Oliver and Boyd. Edinburg, 1963.

[33] Kreith F.: Convection heat transfer in rotating systems. Adv. Heat Transfer, 5, pp.130÷251, 1968.

[34] Meyer R.C.: On reducing aerodynamic heat transfer rates by magnetohydrodynamic techniques. J. Aerospace Sci., 25, pp. 561÷566, 1958.

[35] Rathbun Jr. A.S.: On the flow of an electrically conducting fluid toward a stagnation point in the presence of a magnetic field. Ph. D. Thesis in Mechanical Engineering, University of Pittsburgh, 1961.

[36] Eringen A.C., Maugin G.A.: Electrodynamics of Continua. Vol II, Springer Verlag, 1990.

[37] Gross J.F., Dewey C.F.: Archiwum Mechaniki Stosowancj. 3, 761, 1964.

[38] Wortman A., Ziegler H., Soo-Hoo G.: Convective heat transfer at a general three-dimensional stagnation point. Int. J. Heat Mass Transfer, 14, pp. 149÷152, 1971.

[39] Lee E.S.: Quasilinearization and Invariant Imbedding with Application to Chemical Engineering and Adoptive Control. Academic Press, New York, 1968.

[40] Radbill J.R., McCue G.A.: Quasilinearization and Nonlinear Problems in Fluid and Orbital Mechanics, Elsevier Publishing Company, New York, 1970.

[41] Back L.H.: Flow and heat transfer in laminar boundary layers with swirl. AIAA J., 7, pp. 1781÷1789, 1969.

Przepływ w ściśliwej warstwie granicznej w regionie zastoju dla wirującej kuli przy wielkich szybkościach wtryskiwania i w obecności pola magnetycznego

Streszczenie

W pracy zbadano efekt dużych szybkości wtryskiwania płynu na stabilną, laminarną ściśliwą warstwę graniczną w regionie czołowego punktu zastoju dla wirującej kuli w obecności pola magnetycznego. W analizie uwzględniono efekt zmienności właściwości gazu, efekt rozpraszania lepkiego oraz wpływ różnej od jedności liczby Prandtla. Nieliniowe sprzężone zwyczajne równania różniczkowe, które opisują przepływ, zostały najpierw zlinearyzowane przy zastosowaniu techniki quasi-linearyzacji, a uzyskany stąd układ równań liniowych został rozwiązany bezpośrednią metodą różnic skończonych przy zmiennej długości kroku. Wyrażenia analityczne powierzchniowych naprężeń ścinających w kierunku wzdłużnym i kierunku rotacji, jak i wyrażenia powierzchniowego transferu ciepła, uzyskano dla dużych szybkości wtryskiwania także przy użyciu metody przybliżonej. Dla dużych szybkości wtryskiwania transfer ciepła dąży do zera, lecz powierzchniowe naprężenia ścinające w kierunku wzdłużnym i kierunku rotacji pozostają skończone, choć małe. Powierzchniowe naprężenia ścinające i powierzchniowy transfer ciepła maleją ze wzrostem szybkości wtryskiwania, ale wzrastają z polem magnetycznym i parametrem rotacji. Pole magnetyczne, podobnie jak parametr rotacji, powodują powstanie efektu przerzutu w profilu szybkości wzdłużnej, a wartość tego przerzutu wzrasta znacząco przy zwiększaniu parametrów rotacji i parametrów wtryskiwania. Położenie linii podziału strumienia oddala się od granicy przy wzrastającej szybkości wtryskiwania, lecz zbliża się do niej przy wzroście parametrów rotacji i pola magnetycznego.